



Cite this: RSC Adv., 2016, 6, 20166

Compressive mechanical properties and microstructure of PVA–HA hydrogels for cartilage repair

Wenxu Li,^{*a} Duo Wang,^a Wen Yang^a and Ying Song^b

In this paper, hydroxyapatite (HA) was deposited on poly(vinyl alcohol) (PVA) molecular chains by an *in situ* synthetic method. Subsequently, combining cyclic freeze/thaw treatment, PVA–HA gel composites consisting of flexible PVA and rigid HA were prepared. The phase composition and structure of the PVA–HA hydrogels were investigated by XRD, IR and SEM methods, and their compressive mechanical properties were evaluated using mechanical test equipment. The results showed that PVA provides a flexible porous network skeleton to the hydrogel. The HA particles were distributed inside the pores and on the walls of the pores, strengthening the compressive properties of the PVA–HA hydrogel. Moreover, the increased PVA and HA contents could increase the compressive modulus and compressive strength of the hydrogel. The effect of the PVA content on the compressive mechanical properties of the hydrogel was predominant, especially at high strain rates. The maximum compressive strength of the PVA–HA hydrogel was 0.43 MPa, which remained even at a compression deformation rate up to 70%. The relationship between the compressive modulus and compression ratio tended to be an exponential function, same as the trend of the stress–strain curve. The results indicate that the prepared hydrogel is a viscoelastic material, which has potential for the application of articular cartilage repair.

Received 25th January 2016
Accepted 29th January 2016

DOI: 10.1039/c6ra02166b
www.rsc.org/advances

1 Introduction

Articular cartilage has a very poor ability to self-heal once lesions are induced by joint disease, trauma or natural degeneration. Surgery is needed to repair or replace damaged cartilage, relieving joint pain or restoring the biological and physiological functions of the joints.¹ At present, there is a tremendous amount of research to develop biomimetic and bio-inspired polymer hydrogels in order to facilitate tissue replacement, repair and regeneration because hydrogels with high water content, up to 90%, are usually viscoelastic and resemble the network structure of the natural articular cartilage.² Some kinds of natural or synthetic polymer hydrogel, such as poly(vinyl alcohol) (PVA), collagen and chitosan, have been widely used in artificial cartilage tissue engineering.^{3–6} Of these, PVA hydrogel has good biocompatibility and a high elastic modulus even when the water content is very high,⁷ as well as good physicochemical and excellent biotribological properties.⁸ Thus, the PVA hydrogel has increasingly attracted interest as a biomaterial that might be used to replace diseased or damaged articular cartilage.^{9,10} However, its poor mechanical properties

(strength and toughness) is a major problem, preventing its use to replace articular cartilage.¹¹ Moreover, since the PVA hydrogel does not adhere to tissue, owing to its non-bioactivity, the long-term fixation of PVA hydrogel implant by suturing is difficult.

It has been previously reported that nano-hydroxyapatite has been applied widely in the medical field as a bone repair material because of its similar composition to human hard tissue.^{12,13} Hydroxyapatite-nanocomposites have greater biological efficiency in terms of osteoblast adhesion, proliferation and the formation of new bone on their surfaces.^{14,15} To simulate the tissue structure and chemical composition of the calcified layer in human cartilage, the inorganic component hydroxyapatite was brought into the PVA hydrogel to strengthen its compressive mechanical properties. Meanwhile, the biological activity and osteoinductivity of hydroxyapatite can be used to play an important role in the *in situ* growth and reconstruction of the implanted body parts.^{16–21}

Traditionally, PVA composites were obtained by simple physical mixing. This approach is not able to control the morphology of the materials, and will not initiate the interfacial chemical reactions between organic and inorganic phases; thus, the resulting PVA composites are different from the natural cartilage. Therefore, various kinds of new preparation techniques have been developed in recent years, such as *in situ* co-precipitation method,^{22,23} the sol-gel method,²⁴ supercritical fluid technology,²⁵ and solvent casting technology.²⁶ At present, the *in situ* co-precipitation method has been paid much attention for the synthesis of biomimetic

^aDept. of Chemistry, Harbin Institute of Technology, Harbin 150001, China. E-mail: liwx@hit.edu.cn

^bChemical Engineering and Technology, Harbin Institute of Technology, Harbin, 150001, China

materials^{27,28} because the *in situ* precipitation process for hydroxyapatite on a polymer matrix is similar to the *in situ* mineralization process of hydroxyapatite on natural bone. Some studies on the *in situ* synthesis of nanometer-scale hydroxyapatite in the PVA matrix have been reported.^{11,29,30}

The mineralization of hydroxyapatite in biological systems typically occurs in a hydrogel environment. It is helpful to understand the nature of the hydroxyapatite mineralization for the synthesis in a hydrogel.³¹ In addition, the mechanical strength of the resulting hydrogel can be enhanced by repeated freeze-thaw cycles.³²

The aim of this study was to obtain hydroxyapatite reinforced PVA hydrogels using an *in situ* synthesis method, accompanied by freeze-thaw cycles. The effects of the hydroxyapatite on the microstructures and compressive properties of the PVA-HA hydrogels for use as articular cartilage replacements were also investigated.

2 Material and methods

2.1 Materials

For the synthesis of PVA-HA hydrogels, the following reagents were used. PVA (viscosity-average molecular weight 3.4×10^5 , Tianjin Chemical Reagent Co.), $\text{Ca}(\text{NO}_3)_2 \cdot 4\text{H}_2\text{O}$ (analytical reagent, Tianjin Guangfu Fine Chemical Research Institute), $(\text{NH}_4)_2\text{HPO}_4$ (analytical reagent, Tianjin Dongliqu Tianda Chemical Reagent, Co.), NaOH (analytical reagent, Beijing Yili Fine Chemical Co.) and distilled water.

2.2 Preparation of PVA-HA hydrogels

First, $\text{Ca}(\text{NO}_3)_2 \cdot 4\text{H}_2\text{O}$ was dissolved in distilled water, and PVA was then added to this aqueous solution. After an hour of stirring, a certain concentration of $(\text{NH}_4)_2\text{HPO}_4$ aqueous solution was added drop-by-drop to this solution (for all studied concentrations, a stoichiometric ratio of Ca/P = 1.67 was maintained; this ratio satisfies the synthesis reaction conditions of hydroxyapatite). A milky suspension was obtained, and its pH was adjusted to 9 ± 0.2 with NaOH solution (1 mol L^{-1}). Subsequently, the solution was maintained at 80°C for 12 hours. The mixture was poured into plastic moulds and three cycles of freezing and thawing (freezing at -20°C and thawing at 25°C) were performed for 12 h per stage, to improve the mechanical strength of the PVA-hydroxyapatite hydrogel. The preparation is outlined in Fig. 1.

Preliminary unpublished work conducted in our laboratory involved the synthesis of a range of multicomponent PVA-HA hydrogels. The composition that was selected for the present study, its optimized mechanical properties and microstructure, is shown in Table 1.

2.3 Evaluation of microstructures and mechanical properties

Micrographs were obtained by scanning electron microscopy (HITACHI S-4700). Samples were freeze-dried and gold-coated by ion sputtering. Tests were carried out in the dry stage.

The major functional groups of the PVA-HA hydrogels were identified by infrared spectroscopy (NICOLET 6700). The resolution of the infrared spectroscopy was 4 cm^{-1} . The scanning range was $4000\text{--}400 \text{ cm}^{-1}$.

The crystal structures of inorganic phases distributed in the matrix were determined by X-ray diffraction (Philips Analytical X-ray) using Cu K α radiation at 40 kV and 50 mA. The samples were scanned from $2\theta = 5^\circ$ to $2\theta = 90^\circ$.

The compressive strength of the samples was tested using a universal testing machine Instron 5500R at room temperature with a crosshead speed of 2 mm min^{-1} . The hydrogels were swollen in distilled water before measurement, until the water content reached equilibrium. The samples were made into a cylinder of diameter (ϕ) $27 \text{ mm} \pm 0.5 \text{ mm}$ and height (h) $6 \text{ mm} \pm 1 \text{ mm}$. Because the deformation characteristics of the samples were similar to rubber, test methods of compression performance for rubber were selected to test the compression performance of the hydrogels. The compressive modulus with the compressive strain ratio at 60% was chosen as the compressive strength of the sample. The compressive strength and compressive modulus can be calculated by the following equations.

$$\text{CS} = \frac{F}{S} \quad (1)$$

In eqn (1), F (N) is the force acting on the section of the sample and S (m^2) is the area of the section of the sample.

$$\varepsilon = \frac{\Delta h}{h} \quad (2)$$

In eqn (2), Δh (mm) is the change in height of the sample, h (mm) is the original height of the sample and ε is the compressive strain ratio.³³

$$E_\varepsilon = \frac{\sigma_{\varepsilon+\Delta\varepsilon} - \sigma_{\varepsilon-\Delta\varepsilon}}{2\Delta\varepsilon} \times 100\% \quad (3)$$

In eqn (3), ε is the compressive strain ratio and E_ε is the compressive modulus of the hydrogel for compressive strain ratio ε . The value of $\Delta\varepsilon$ is 1%. $\sigma_{\varepsilon+\Delta\varepsilon}$ is the pressure when the compressive strain ratio is $\varepsilon + \Delta\varepsilon$ and $\sigma_{\varepsilon-\Delta\varepsilon}$ is the pressure when the compressive strain ratio is $\varepsilon - \Delta\varepsilon$.

3 Results and discussion

3.1 Phase of the PVA-HA hydrogels

Fig. 2 shows the X-ray diffraction patterns of the hydroxyapatite, PVA and PVA-HA hydrogels. It is well known that the PVA polymer exhibits a semi-crystalline structure with a large peak at $2\theta = 19\text{--}20^\circ$ and a small peak at $39\text{--}40^\circ$.^{34,35} This confirms that there is crystalline hydroxyapatite and semi-crystalline PVA in the hydrogel. The diffraction peaks at 31.7° , 32.1° and 32.8° correspond well with the salient peak of hydroxyapatite (PDF 09-432).

Moreover, it is clearly seen that the characteristic peak intensities of hydroxyapatite for P6H1 and P2H1 are greatly reduced compared with that for P2H4. This finding indicates

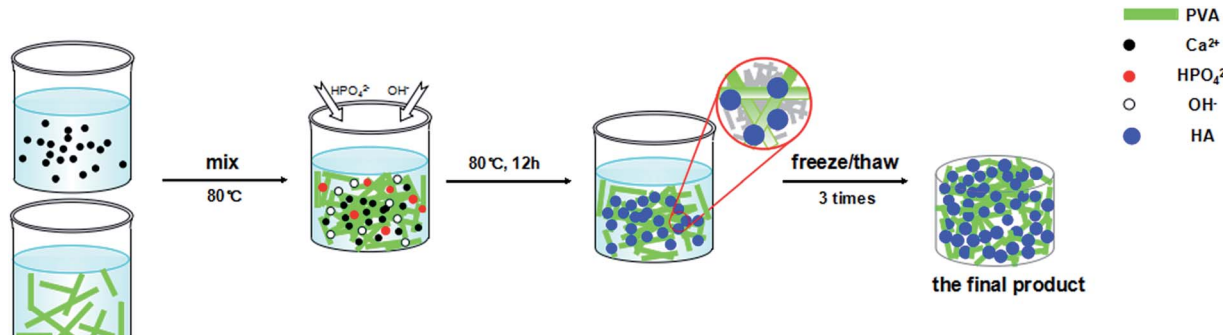


Fig. 1 Schematic showing the synthetic steps.

that the degree of crystallinity of hydroxyapatite in the PVA–HA hydrogels decreases with a decrease in inorganic salt concentration and an increase in PVA concentration.

Fig. 3 shows the FTIR spectra of the PVA–HA hydrogels and Table 2 shows the main absorption peaks and the corresponding functional groups. In the spectrum of hydroxyapatite, the peak at 1035 cm^{-1} indicates the symmetrical stretching vibration of the P–O bond in PO_4^{3-} , and the peak at 1117 cm^{-1} indicates the anti-symmetrical stretching vibration of the P–O bond. In CO_3^{2-} , the wavenumber corresponding to the stretching vibration of the C–O bond is 1387 cm^{-1} , and the peak at 3573 cm^{-1} indicates the stretching vibration of hydroxyl groups ($-\text{OH}$). In the spectrum of PVA, the peak at 3268 cm^{-1} is the characteristic peak of hydroxyl groups ($-\text{OH}$). The peaks at 2920 cm^{-1} and 2850 cm^{-1} both indicate the stretching vibration of the C–H bond. The peak at 1558 cm^{-1} indicates the stretching vibration of the C=O bond in polyvinyl acetate (the precursor of PVA). The peaks at 1417 cm^{-1} and 1326 cm^{-1} indicate the deformation vibration of the C–O bond, while that at 1085 cm^{-1} indicates the stretching vibration. The peak at 1144 cm^{-1} indicates the characteristic absorption peak of the C–C bond.^{36,37}

In the FTIR spectra of the PVA–HA hydrogels, the absorption peaks of PVA and hydroxyapatite can both be observed. With the increasing content of PVA and the decreasing content of the inorganic salt, the absorption peak intensity of PVA gradually increases, and that of hydroxyapatite decreases. Hydrogen bonding between hydroxyl groups of hydroxyapatite molecules and PVA chains decreases the concentration of hydroxyl groups in the hydrogel. In the spectra, the intensities of peaks indicating the vibration of hydroxyl groups at 3573 cm^{-1} and 3268 cm^{-1} are weaker than those of pure hydroxyapatite and PVA. Moreover, the position of these peaks is slightly left-shifted to 3279 cm^{-1} compared with the peak for pure PVA (3268 cm^{-1}).

Table 1 Design of material component

Samples	Content of PVA (wt%)	Content of $\text{Ca}(\text{NO}_3)_2$ (mol L^{-1})	Content of $(\text{NH}_4)_2\text{HPO}_4$ (mol L^{-1})
P2H4	2	0.24	0.144
P2H1	2	0.06	0.036
P6H1	6	0.06	0.036

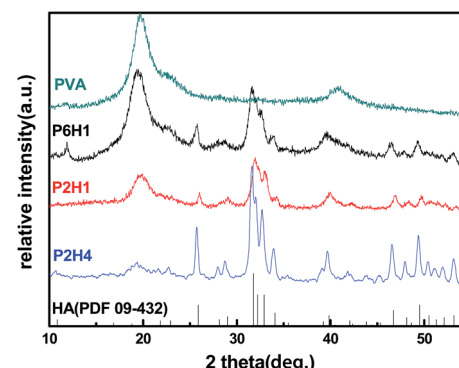


Fig. 2 XRD patterns of PVA–HA hydrogels.

This indicates that the hydrogen bond interaction between PVA and hydroxyapatite through hydroxyl groups leads to the development of physical crosslinking.

3.2 Microstructure of PVA–hydroxyapatite hydrogels

The hydrogels were uniform milky white, smooth and elastic, as shown in Fig. 4. The effects of the material components on the microstructure can be investigated by scanning electron microscopy (Fig. 5). It can be seen that the PVA–HA hydrogels consisted of flexible PVA and rigid hydroxyapatite.

A hydroxyl group in PVA molecules leads to the development of hydrogen bonding of intra- and inter-PVA molecular chains. These hydrogen bonds lead to physical crosslinking of the PVA,^{38,39} leading to the fabrication of a three-dimensional network.⁴⁰ Therefore, the network morphology of hydrogels with different PVA contents could be observed.

Moreover, the dispersed PVA molecular chain could be used as a stencil, onto which Ca^{2+} was attracted and held by Coulomb forces to ensure that PO_4^{3-} could be combined with Ca^{2+} , initiating the nucleation of hydroxyapatite,⁴¹ followed by the growth of hydroxyapatite particles on the organic polymer.

When the content of inorganic salts is higher (P2H4 in Fig. 5a), many hydroxyapatite particles accumulate in the network and occupy the majority of the pores, owing to the higher content of Ca^{2+} and PO_4^{3-} . As a result, the characterization of porous networks in the microstructure is not obvious.

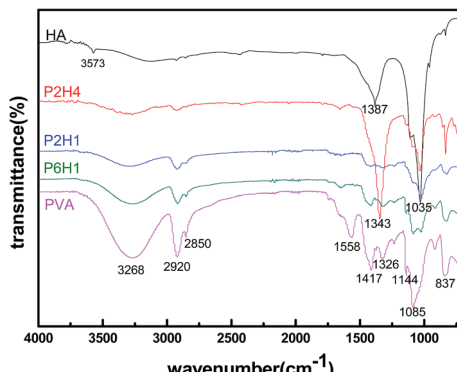


Fig. 3 FTIR spectra of PVA–HA hydrogels.

With decreasing inorganic salt concentration, the amount of hydroxyapatite reduces (P2H1 in Fig. 5b). The network formed by the PVA gel can clearly be seen, and the network wall becomes thinner. The pore size is about 1–5 μm . A few hydroxyapatite particles on the polymer surface were also observed.

On further increasing the concentration of PVA (P6H1 in Fig. 5c), the extent of crosslinking between PVA molecular chains is increased. As a result, the walls of pores in the network of the hydrogel become thicker and the diameters of the pores decrease. In addition, the growth of the hydroxyapatite particles in the hydrogel is suppressed, leading to the disappearance of hydroxyapatite particles from the surface of the hydrogel.

3.3 Compression mechanical properties of PVA–HA hydrogels

3.3.1 Stress-strain characteristics of PVA–HA hydrogels. Fig. 6 shows the stress–strain curve of the PVA–HA hydrogels. As shown in the figure, the relationship between stress and strain is nonlinear. Simulation using Origin 8.0 demonstrates that the stress–strain behaviours of all the hydrogels fit an exponential relationship, with a correlation coefficient R^2 of more than 0.999. This kind of exponential relationship could explain the special viscoelasticity, which is not destroyed even when the compression deformation is as high as 70%.

The three-dimensional network structure in the hydrogel holds the amorphous and microcrystalline regions of PVA, the hydroxyapatite particle reinforcing phase and lots of free water, which enable the flexible PVA molecular chains to respond rapidly to external forces by rearranging themselves simultaneously, ultimately resulting in the relatively high compressive



Fig. 4 Photograph of PVA–HA hydrogel.

strain ratio of the hydrogel. Moreover, both the free water and the amorphous regions in the hydrogel are beneficial to the viscous characteristics of the hydrogel.³³

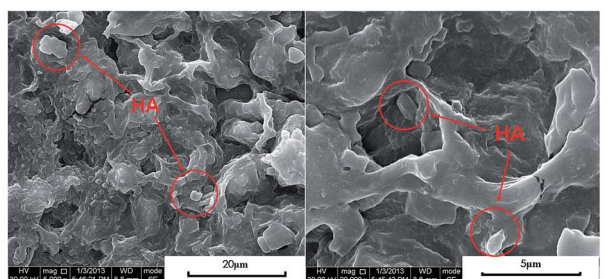
In addition, at every compressive strain level, the sample with the higher content of hydroxyapatite (P2H4) and that with the higher content of PVA (P6H1) exhibited larger compressive stress. For example, when the strain ratio is 50%, the compressive stress of the hydrogel rises from 0.08 MPa (P2H1) to 0.12 MPa (P2H4) with increasing hydroxyapatite content. The compressive stress of the hydrogel rises rapidly from 0.08 MPa (P2H1) to 0.22 MPa (P6H1) with increasing PVA content.

It can be seen that the increasing content of hydroxyapatite or PVA in hydrogels can help to improve the compression performance of the hydrogels. However, the effect of the increasing content of PVA on the hydrogel stress–strain curve of hydrogels is more predominant, especially at high strain rates. For example, when the strain ratio is 30%, the compressive stresses of the P2H1 and P6H1 are 0.05 MPa and 0.02 MPa, respectively. The compressive stress of the hydrogels is improved by 0.03 MPa with the increasing content of PVA. When the strain ratio increases to 70%, the compressive stresses of the P2H1 and P6H1 are 0.36 MPa and 0.84 MPa, respectively. The compressive stress of the hydrogels is improved by 0.48 MPa.

3.3.2 Compressive strength of PVA–HA hydrogels. In the compressive strength test, it is difficult to crush the sample when measuring the compressive strength, owing to the excellent deformability of the PVA–HA hydrogels. In this case, the sample is compressed to 40% of the original size, that is, the compressive modulus with the compressive strain ratio at 60%

Table 2 The position of the main characteristic peaks and the respective functional group of PVA–HA hydrogels (unit: cm^{-1})

Samples	O–H	C–H	C=O	C–O	C–C	P–O
HA	3573	—	—	1387	—	1117, 1035
P2H4	3285	2924, 2851	—	1343, 1097	1142	1035
P2H1	3289	2924, 2851	—	1420, 1320, 1092	1144	1028
P6H1	3280	2915, 2855	—	1421, 1324, 1088	1146	1026
PVA	3268	2920, 2850	1558	1417, 1326, 1085	1144	—



(a) P2H4

(b) P2H1

(c) P6H1

Fig. 5 Microstructures of PVA-HA hydrogels.

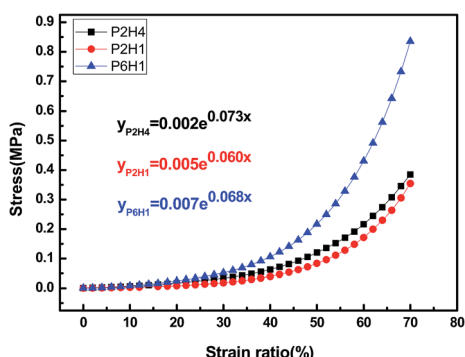


Fig. 6 Stress-strain behavior curves of PVA-HA hydrogels.

is chosen to be the compressive strength of the samples,³³ as shown in Table 3. As seen from the data in the table, the compressive strength of P2H1 is 0.17 MPa, while the compressive strength of P2H4 (the content of inorganic salt increased four times) is 0.22 MPa. The compressive strength increased about 29.4%. The compressive strength of P6H1 (the content of PVA increased three times) is 0.43 MPa. The compressive strength is increased about 153%.

Table 3 Components and compressive strength of PVA-HA hydrogels

Samples	PVA (wt%)	$\text{Ca}(\text{NO}_3)_2$ (mol L ⁻¹)	$(\text{NH}_4)_2\text{HPO}_4$ (mol L ⁻¹)	Compressive strength (MPa)
P2H4	2	0.24	0.144	0.22
P2H1	2	0.06	0.036	0.17
P6H1	6	0.06	0.036	0.43

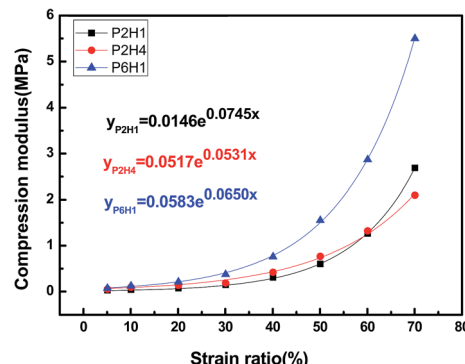


Fig. 7 Changing curves of PVA-HA hydrogels modulus with compression ratios.

In the hydrogel, PVA and hydroxyapatite were combined by intramolecular and intermolecular hydrogen bonding.⁴¹ Increasing the content of PVA and hydroxyapatite will enhance the function of the hydrogen bonding in the hydrogel. Thus, the mechanical properties of the hydrogel were effectively improved. In addition, the rigid hydroxyapatite inorganic reinforcing particles also have good mechanical strength.⁴² It can be seen in the photos of the microstructure in Fig. 5c that, as the concentration of PVA increases, the three-dimensional network skeleton of the hydrogel becomes thicker, leading to an increase in compression performance of the hydrogel.

3.3.3 Compressive modulus of elasticity of PVA-HA hydrogels. Fig. 7 shows the changing trend of the compressive modulus of PVA-HA hydrogels. Simulation using Origin 8.0 demonstrates that the compressive modulus of the hydrogels increases exponentially with increasing compression ratio. This indicates that the compressive modulus depends significantly on the compression ratio. When the content of PVA is 6 wt% and the strain ratio rises from 5% to 60%, the compressive modulus of PVA-hydroxyapatite hydrogels rises rapidly from 0.07 MPa to 2.86 MPa, increasing 40 times.

Once the load is applied, the polymeric chains of the hydrogel are reoriented with changed relative positions, while the free water begins to drain and escapes from the hydrogel. It is possible to achieve a significant deformation for the application of a relatively small load. When it is experiencing low strain ratios, the hydrogel exhibits excellent deformability and the lower compressive modulus, owing to the three-dimensional pore structure of PVA and the free water contained in the network structure of the hydrogel.

When the application of the load continues to high strain ratios, the orientation of the PVA chains tends to become uniform, while the friction caused by the flow of free water begins to produce a hardening effect on the hydrogel. Furthermore, the presence of hydroxyapatite reinforcing particles resists deformation of the hydrogel. As a result, the hydrogel presents significant anti-deformability and obviously increased compressive modulus.^{11,43}

The compressive modulus of the hydrogel increases exponentially with the increase in compression ratio; this is similar to the response of natural cartilage.^{11,33} Under low compressive stress, the compressive stress can be uniformly distributed by enlarging the contact area of the articular cartilage. When the natural articular cartilage is under considerably high stress, e.g., when running and jumping, the compressive modulus increases exponentially to resist the high compressive stress, reducing deformation and preventing the cartilage damage.

Further studies relating to the degree of swelling, and the mechanical and water absorption properties of PVA-HA hydrogels with different hydroxyapatite contents are being conducted.

4 Conclusions

PVA-HA gel composites consisting of flexible PVA and rigid hydroxyapatite were prepared by *in situ* synthesis accompanied by freeze-thaw cycles. The PVA hydrogel forms a porous network, and the hydroxyapatite particles distributed in the PVA matrix play a role in strengthening the compressive properties of the hydrogels. The increasing content of the PVA and hydroxyapatite could improve the elastic modulus and compressive strength of the hydrogels. The effect of the PVA content on the compressive properties of the hydrogels is more obvious, especially at high strain rates. The maximum compressive strength of the hydrogel is 0.43 MPa (P6H1), and the sample could not be destroyed even when the compression deformation reached 70%, indicating that PVA-HA hydrogel is a viscoelastic material. The relationship between the compressive modulus and the compression ratio of the hydrogels is exponential, and the stress-strain curve shows the same trend. The responses of the hydrogels to different levels of external stress are similar to those of natural articular cartilage.

Acknowledgements

This work was financially supported by the projects of 2013 science and technological innovation platform in the field of manufacturing and key scientific and technological projects of Heilongjiang Province (grant no. GC13A102), China.

References

- W. Zhao, X. Jin, Y. Cong and Y. Y. Liu, *J. Chem. Technol. Biotechnol.*, 2013, **88**, 327–339.
- Q. Wang, R. X. Hou and Y. J. Cheng, *Soft Matter*, 2012, **8**, 6048–6056.
- E. A. Appel, J. Barrio and X. J. Loh, *Chem. Soc. Rev.*, 2012, **41**, 6195–6214.
- J. Y. Sun, X. H. Zhao and W. R. K. Illeperuma, *Nature*, 2012, **489**, 133–136.
- R. Jin, T. L. S. Moreira and P. J. Dijkstra, *Biomaterials*, 2009, **30**(13), 2544–2551.
- K. S. Stok, G. Lisignoli and S. Cristina, *J. Biomed. Mater. Res., Part A*, 2010, **93**(1), 37–45.
- M. Kobayashi, Y. S. Chang and M. Oka, *Biomaterials*, 2005, **26**, 3243–3248.
- Y. Pan, D. Xiong and X. Chen, *Key Eng. Mater.*, 2007, **330**–332, 1297–1300.
- V. M. Sardinha, L. L. Lima, W. D. Belangero, C. A. Zavaglia, V. P. Bavaresco and J. R. Gomes, *Wear*, 2013, **301**, 218–225.
- J. A. Stammen, S. Williams and D. N. Ku, *Biomaterials*, 2001, **22**, 799–806.
- S. Maiolo, M. Amado and J. Gonzalez, *Mater. Sci. Eng., C*, 2012, **32**, 1490–1495.
- H. Tamagawa, T. Tenkomo and T. Sugaya, *Appl. Surf. Sci.*, 2012, **262**, 140–145.
- C. C. Zhou, C. Y. Deng and X. N. Chen, *J. Mech. Behav. Biomed. Mater.*, 2015, **48**, 1–11.
- A. Gupta, G. Tripathi and D. Lahiri, *J. Mater. Sci. Technol.*, 2013, **29**(6), 514–522.
- S. C. Chao, M. J. Wang and N. S. Pai, *Mater. Sci. Eng., C*, 2015, **57**, 113–122.
- B. Cengiz, Y. Gokce and N. Yildiz, *Colloids Surf., A*, 2008, **322**(1–3), 29–33.
- R. X. Hou, L. Nie and G. L. Du, *Colloids Surf., B*, 2015, **132**, 146–154.
- F. Chen, Q. L. Tang and Y. J. Zhu, *Acta Biomater.*, 2010, **6**(8), 3013–3020.
- A. Tampieri, S. Sprio and M. Sandri, *Trends Biotechnol.*, 2011, **29**(10), 526–535.
- Z. Lu, Y. Liu and B. Liu, *Mater. Des.*, 2012, **39**, 444–449.
- M. R. Nikpour, S. M. Rabiee and M. Jahanshahi, *Composites, Part B*, 2012, **43**(4), 1881–1886.
- C. Katepetch and R. Rujiravanit, *Carbohydr. Polym.*, 2011, **86**(1), 162–170.
- W. Y. Choi, H. E. Kim and S. Y. Oh, *Mater. Sci. Eng., C*, 2010, **30**(5), 777–780.
- X. M. Shi, S. M. Xu and J. T. Lin, *Mater. Lett.*, 2009, **63**(5), 527–529.
- C. Delabarde, C. J. G. Plummer, P. Bourban and J. E. Månsen, *Polym. Degrad. Stab.*, 2011, **96**(4), 595–607.
- E. Wenk, A. J. Meinel and S. Wildy, *Biomaterials*, 2009, **30**(13), 2571–2581.
- A. Rezaei and M. R. Mohammadi, *Mater. Sci. Eng., C*, 2013, **33**(1), 390–396.
- A. Rogina, P. Rico and G. G. Ferrer, *Eur. Polym. J.*, 2015, **68**, 278–287.
- F. L. Xu, Y. B. Li and X. J. Wang, *J. Mater. Sci.*, 2004, **39**, 5669–5672.
- S. Mollazadeh, J. Javadpour and A. Khavandi, *Adv. Appl. Ceram.*, 2007, **106**(4), 165–170.
- B. Q. Li and Y. L. Wang, *J. Biomater. Sci., Polym. Ed.*, 2011, **22**, 505–517.

- 32 W. Song, D. C. Markel and X. Jin, *J. Biomed. Mater. Res., Part A*, 2012, **100**(11), 3071–3079.
- 33 Y. S. Pan and D. S. Xiong, *J. Mater. Sci.: Mater. Med.*, 2009, **20**, 1291–1297.
- 34 R. Ricciardi, F. Auriemma and C. D. Rosa, *Macromolecules*, 2004, **37**(5), 1921–1927.
- 35 C. C. Yang, C. T. Lin and S. J. Chiu, *Desalination*, 2008, **233**, 137–146.
- 36 M. M. Blum and T. C. Ovaert, *J. Biomed. Mater. Res., Part B*, 2012, **100**, 1755–1763.
- 37 S. A. Poursamar, M. Azami and M. Mozafari, *Colloids Surf., B*, 2011, **84**, 310–316.
- 38 G. Paradossi, F. Cavalieri, E. Chiessi and C. Spagnoli, *J. Mater. Sci.: Mater. Med.*, 2003, **14**(8), 687–691.
- 39 J. A. Stammen, S. Williams and D. N. Ku, *Biomaterials*, 2001, **22**(8), 799–806.
- 40 H. E. Assender and A. H. Windle, *Polymer*, 1998, **39**(18), 4303–4312.
- 41 F. L. Xu and X. J. Wang, *J. Mater. Sci.*, 2004, **39**, 5669–5672.
- 42 J. A. Stammen, S. Williams and D. N. Ku, *Biomaterials*, 2001, **22**(8), 799–806.
- 43 S. Park, C. T. Hung and G. Ateshian, *Osteoarthritis Cartilage*, 2004, **12**, 65–72.